JOURNAL OF NEUROTRAUMA 34:1412–1426 (April 1, 2017)

DOI: 10.1089/neu.2016.4581

Resting-State Magnetoencephalography Reveals Different Patterns of Aberrant Functional Connectivity in Combat-Related Mild Traumatic Brain Injury

Ming-Xiong Huang,[1,2] Deborah L. Harrington,[1,2] Ashley Robb Swan,[1,2] Annemarie Angeles Quinto,[1,2] Sharon Nichols,[3] Angela Drake,[4] Tao Song,[2] Mithun Diwakar,[2] Charles W. Huang,[5] Victoria B. Risbrough,[6,7] Anders Dale,[2] Hauke Bartsch,[2] Scott Matthews,[1,6,8] Jeffrey W. Huang,[9] Roland R. Lee,[1,2] and Dewleen G. Baker,[1,6,7]

Abstract

Blast mild traumatic brain injury (mTBI) is a leading cause of sustained impairment in military service members and veterans. However, the mechanism of persistent disability is not fully understood. The present study investigated disturbances in brain functioning in mTBI participants using a source-imaging-based approach to analyze functional connectivity (FC) from resting-state magnetoencephalography (rs-MEG). Study participants included 26 active-duty service members or veterans who had blast mTBI with persistent post-concussive symptoms, and 22 healthy control active-duty service members or veterans. The source time courses from regions of interest (ROIs) were used to compute ROI to whole-brain (ROI-global) FC for different frequency bands using two different measures: 1) time-lagged cross-correlation and 2) phase-lock synchrony. Compared with the controls, blast mTBI participants showed increased ROI-global FC in beta, gamma, and low-frequency bands, but not in the alpha band. Sources of abnormally increased FC included the: 1) prefrontal cortex (right ventromedial prefrontal cortex [vmPFC], right rostral anterior cingulate cortex [rACC]), and left ventrolateral and dorsolateral prefrontal cortex; 2) medial temporal lobe (bilateral parahippocampus, hippocampus, and amygdala); and 3) right putamen and cerebellum. In contrast, the blast mTBI group also showed decreased FC of the right frontal pole. Group differences were highly consistent across the two different FC measures. FC of the left ventrolateral prefrontal cortex correlated with executive functioning and processing speed in mTBI participants. Altogether, our findings of increased and decreased regionalpatterns of FC suggest that disturbances in intrinsic brain connectivity may be the result of multiple mechanisms, and are associated with cognitive sequelae of the injury.

Keywords: blast brain injury; excitation; inhibition; FC; MEG; TBI

Introduction

Blast related traumatic brain injury (TBI) is a leading cause of sustained physical, cognitive, emotional, and behavioral deficits in military service members and veterans. Of TBIs in which blast was the main cause in active-duty military personnel and veterans wounded in combat in Iraq and Afghanistan, the majority (89%) were mild TBIs (mTBI).[1] However, the pathophysiology of blast mTBI is not completely understood, and the long-term effects of mTBI in general are controversial. In the majority of individuals with mTBI, symptoms resolve within days post injury.[2] However, post-concussive symptoms (PCS) can persist for 3 months post-injury or longer, indicating chronic sequelae. Estimates of the prevalence of persistent PCS vary widely, particularly in veterans with mTBI, with at least three enduring PCS reported in 7.5–40% of patients.[3–6] At present, it is unclear why similar acute mTBI events can lead to dramatic neurobehavioral decompensation with persistent PCS in some individuals, but not in others.[7] Optimal rehabilitation treatments for blast mTBIs are also unknown, in part because of insufficient information about the loci and mechanisms of the injury. Conventional neuroimaging techniques have limited sensitivity to detect physiological alterations

[1]Radiology, Research, and Psychiatry Services, VA San Diego Healthcare System, San Diego, California.
Departments of [2]Radiology, [3]Neuroscience, [5]Bioengineering, and [6]Psychiatry, University of California, San Diego, California.
[4]Naval Medical Center, San Diego, California.
[7]VA Center of Excellence for Stress and Mental Health, San Diego, California.
[8]Aspire Center, VASDHS Residential Rehabilitation Treatment Program, San Diego, California.
[9]Westview High School, San Diego, California.

caused by mTBI, as mild and some moderate TBIs are often not visible on conventional acute MRI or CT,[8–10] even in individuals with persistent PCS and cognitive deficits. This highlights the limited value of conventional CT and MRI in assessing the loci and mechanisms of blast mTBI, and the need for techniques that are sensitive to the effects of blast exposure on the brain and the efficacy of therapeutic interventions aimed at improving functional capacity.

Identifying and assessing neuropathological, cellular, cognitive, emotional, behavioral and neurological consequences of blast TBI have been challenging.[11] Although this is a topic of debate, it has been suggested that blast TBI is a new subtype of TBI, different from blunt TBI.[11,12] However, there is no debate that blast TBI has some unique injury mechanisms.[13] Specifically, the signature TBI has changed from penetrating injuries during the Vietnam War to blast-induced TBI in contemporary warfare, with the use of improvised explosive devices (IED). At the same time, new equipment for body protection has increased the survival rate after TBI on the battlefield. A blast injury is a complex type of physical trauma and includes a variety of injuries, but the majority of blast induced TBI fall into the category of mTBI.[14] It is important to underscore the different physics in blast TBI and blunt force TBIs such as those most commonly seen in civilian settings. Extreme forces and their complex propagation characterize blast TBI.[15] Injury from blast can result from secondary, tertiary, and even quaternary effects as well as the primary supersonic pressure wave produced by the blast, all of which have been studied in brain injury models. Secondary effects, caused by the impact of flying objects, such as shrapnel fragments, can generate penetrating injuries. Tertiary effects of blast resulting from acceleration/deceleration trauma may also produce tissue shearing and diffuse injuries. Quaternary effects of blast result from heat, smoke, or emission of electromagnetic pulses from detonations.[16]

Measures of functional connectivity (FC) are of keen interest in mTBI because they are sensitive to disturbances in the communication among brain regions. Although disturbances in FC have been reported in many studies of mTBI, there are large discrepancies in the findings. For example, out of 25 resting-state functional magnetic resonance imaging (rs-fMRI) studies of mTBI, 6 showed only increased FC,[17–22] 9 showed only decreased FC,[23–32] and 10 showed both increased FC in some brain networks/regions and decreased FC in other networks/regions.[33–41] Twenty-one of these rs-fMRI studies were concerned with blunt mTBI whereas only four were related to blast mTBI. In the four blast mTBI studies, Gilmore and colleagues found reduced FC between visual network regions and other brain areas,[23] Robinson and colleagues found decreased FC of bilateral primary somatosensory and motor cortices,[28] Han and colleagues found increased within-module FC, but decreased inter-module FC,[33] and Vakhtin and colleagues found decreased FC among various brain networks (default mode network [DMN]-basal ganglia, attention-sensorimotor, frontal-DMN, attention-frontal, and sensorimotor-sensorimotor).[32] The reasons for these discrepant findings is unclear, but may partially relate to the use of different analytic approaches. In addition, Eklund and colleagues recently demonstrated that findings from fMRI studies may be confounded by substantially higher false-positive rates than previously recognized (up to 70% compared with the nominal 5%) because of an unintended artifact of widely used software packages.[42]

However, discrepancies in FC are not unique to studies using indirect measures of neuronal activity such as fMRI. Discrepancies in patterns of aberrant intrinsic activity in mTBI also exist among studies using magnetoencephalography (MEG), which directly measure neuronal activity in gray matter (GM). The excellent temporal resolution of MEG (<1 ms), together with its high spatial localization accuracy (2–3 mm cortex),[43] render it well suited for analyzing FC in different frequency bands, which can potentially provide insight into underlying pathological processes. MEG is highly sensitive to abnormal slowing of signals within the delta band (1–4 Hz) and theta band (5–7 Hz) in mTBI.[44–49] There have been only a few resting state MEG (rs-MEG) studies of FC changes in TBI. Tarapore and colleagues found decreased FC of frontal and parietal-temporal-occipital regions in a mixed sample of mild, moderate, and severe TBI,[50] whereas Alhourani and colleagues reported decreased FC in band-specific networks (e.g., DMN) in mTBI.[51] Applying graph theory-based analyses to sensor waveform cross-frequency coupling measures, Antonakakis and colleagues found decreased global efficiency, but increased local efficiency in mTBI.[52] In contrast, Dimitriadis and colleagues, who also used graph theory analysis, reported decreased local FC and increased long-range FC in mTBI.[53] The latter finding is compatible with those of Dunkley and colleagues who also found increased long-range FC in the low-frequency band in mTBI.[54] We are not aware of any rs-MEG FC studies of blast mTBI.

In the present study, we sought to identify regional patterns of aberrant whole-brain FC in blast mTBI patients using rs-MEG. Active-duty military service members and veterans with blast mTBI and a healthy control group of military service members and veterans with combat experience underwent rs-MEG recordings. FC in different frequency bands from any given brain area or region of interest (ROI) to the rest of the GM areas (i.e., ROI-global FC) was compared between the two groups. Based on the past research, we predicted that abnormal decreases and increases in FC would be found in blast mTBI patients, possibly because of multiple co-occurring mechanisms for brain disturbances. The relationship between abnormal FC in the mTBI group and neuropsychological measures was also examined, to determine the sensitivity of regional FC disturbances to variations in cognitive functioning.

Methods

The study protocol was approved by institutional review boards of the VA San Diego Healthcare System and Naval Health Research Center at San Diego. All participants gave written informed consent prior to study procedures. The informed consent followed the ethical guidelines of the Declarations of Helsinki (sixth revision, 2008).

Research subjects

Demographic characteristics of participants are listed in Table 1A. Study participants included 26 individuals who had a chronic or subacute blast mTBI with persistent PCS for an average of 16.68 months. Participants with documented blast mTBI were United States active-duty military service members or Operation Enduring Freedom (OEF)/Operation Iraqi Freedom (OIF) veterans with injuries caused by blast exposure during combat or military training. We also recruited 22 healthy control subjects with combat experience (active-duty military service members or OEF/OIF veterans), but without significant history of concussion based on self-report. There were no significant group differences in age or education.

All participants with mTBI were evaluated in a clinical interview to assess the nature of their injuries and persistent PCS. The diagnosis and classification of mTBI participants were based on standard Veterans Administration (VA) and Department of Defense (DOD) diagnostic criteria.[55] Inclusion criteria for mTBI participants included the following: 1) loss of consciousness (LOC) <30 min or transient confusion, disorientation, or impaired consciousness immediately after the trauma; 2) post-traumatic amnesia (PTA) <24 h; and 3) an initial Glasgow Coma Scale (GCS)[56]

Table 1A. Demographic Characteristics in the Control and Blast mTBI Groups

	Control group		*mTBI group*			
	Mean	*SD*	*Mean*	*SD*	p *value*	*Cohen's* d
Age	27.04	5.62	28.41	4.50	0.353	–0.28
Years of education	12.64	0.90	12.77	1.70	0.732	–0.10
Months post-injury			16.68	19.70		
Gender (% males)	100%		100%			

between 13 and 15 (if available). Because the GCS assessment was often not available in theater, individuals with missing GCS, but who met other inclusion criteria, were also enrolled. As for the duration of LOC in mTBI participants, 26.9% of participants reported that they were altered/dazed, 23.1% reported LOC for <1 min, 23.1% reported LOC for 2–15 min, and 26.9% reported LOC for 15–30 min. Regarding the duration of PTA, 15.3% of mTBI participants reported 0–15 min PTA, 50% reported 16–30 min PTA, and 34.7% reported 31 min to 24 h PTA. The majority of participants experienced one mTBI (53.8%), 34.6% reported two or three mTBIs, and 11.5% reported four or five mTBIs. Few participants provided GCS information, because GCS was not recorded or accessible for most blast mTBI participants who received their injury in theater.

In an interview, PCS in all mTBI participants were assessed in 21 categories, modified slightly from the Head Injury Symptom Checklist (HISC[57]): 1) headaches, 2) dizziness, 3) fatigue, 4) memory difficulty, 5) irritability, lack of patience, losing temper easily, 6) anxiety, 7) trouble with sleep, 8) hearing difficulties, 9) blurred vision or other visual difficulties, 10) personality changes (e.g., social problems), 11) apathy, 12) lack of spontaneity, 13) affective lability (quickly changing emotions), 14 depression, 15) trouble concentrating, 16) being bothered by noise, 17) being bothered by light, 18) coordination and balance problems, 19) motor difficulty, 20) difficulty with speech, and 21) numbness/tingling. Only participants with persistent symptoms in at least three of the abovementioned categories were recruited into this study. The number of PCS noted ranged between 4 and 12 (mean = 6.88; SD = 1.95). Table 1B lists the percentages of the mTBI participants and separately the controls who noted each symptom. Although controls were asked about these symptoms, they did not mention having a TBI. Hence, symptoms in control subjects were unrelated to TBI.

Exclusion criteria for study participation were as follows: 1) history of other neurological, developmental, or psychiatric disorders (e.g., brain tumor, stroke, epilepsy, Alzheimer disease, or schizophrenia, bipolar disorder, or diagnosis of learning disability); 2) diagnosis of post-traumatic stress disorder (PTSD) based on a Clinician Administered PTSD scale score (CAPS) ≥30 total score; 3) diagnosis of major depression disorder (MDD) prior to the mTBI; 4) substance or alcohol abuse according to *Diagnostic and Statistical Manual of Mental Disorders*, 5th ed. (DSM-5) criteria within the 6 months prior to the study, based on a clinical interview; 5) history of metabolic or other diseases known to affect the central nervous system;[58] 6) extensive metal dental hardware (e.g., braces and large metal dentures, fillings were acceptable) or other metal objects in the head, neck, or face areas that cause artifacts in the MEG data, not removable during pre-processing; 7) currently taking certain medications (e.g., some sedative neuroleptics and hypnotics) known to alter the power of brain rhythms;[59] 8) suicidal ideation as evaluated using the Beck Depression Inventory (BDI-II), that is, any participant reporting a score of ''2'' or ''3'' on the BDI–II: item 9 (suicidal thoughts or wishes), confirmed in follow-up risk assessment; and 10) previous diagnosis of attention-deficit/hyperactivity disorder (ADHD) or learning disorders.

For mTBI participants who were taking medications that might globally change brain activity such as neuroleptic sedatives, antidepressants, and hypnotics,[59] we sought permission from the patient's treating physician to discontinue the medications five half-lives prior to MEG examinations. If the treating physician denied the request, the participant was not enrolled in the study. No controls were taking medications. Past history of drug and alcohol use were asked about in a detailed screening interview. Participants with previous substance abuse were excluded from the study. Additionally, participants were asked to refrain from drinking alcohol the night before the scan.

Neuropsychological examinations

Neuropsychological tests (Table 2) focused on the assessment of executive functions (Kaplan Executive Function System [D-KEFS] Trail Making Test and Verbal Fluency Test[60]), and processing speed (Symbol Search and Digit Symbol Coding subtests from the Wechsler Adult Intelligence Scale[WAIS][61,62]), which are sensitive to cognitive changes in mTBI (see cited references in article by Robb Swan and coworkers[49]) The D-KEFS Trail

Table 1B. Percentage of Subjects Showing Individual Symptoms in mTBI|Control Groups

Headaches 84.6% | 4.5%	Dizziness 65.4% | 0%	Fatigue 50.0% | 9.1%
Memory difficulty 88.5% | 9.1%	Irritability 76.9% | 13.6%	Anxiety 38.5% | 0%
Trouble with sleep 76.9% | 4.5%	Hearing difficulties 73.1% | 13.6%	Blurred vision and other visual difficulties 11.5% | 0%
Personality changes 15.4% | 4.5%	Apathy 3.8% | 0%	Lack of spontaneity 3.8% | 0%
Affective lability 23.1% | 4.5%	Depression 7.7% | 4.5%	Trouble concentrating 19.2% | 9.1%
Being bothered by noise 0% | 0%	Being bothered by light 3.8% | 4.5%	Coordination/balance problems 26.9% | 4.5%
Motor difficulty 3.8% | 0%	Difficulty with speech 3.8% | 4.5%	Numbness/tingling 11.5% | 0%

mTBI, mild traumatic brain injury.

Table 2. Neuropsychological Test Performance in the Control and Blast mTBI Groups

	Control group		*mTBI group*			
	Mean	*SD*	*Mean*	*SD*	p *value*	*Cohen's* d
D-KEFS Trail Making Test						
Visual Scanning	10.67	2.80	10.08	3.04	0.432	0.21
Number Sequencing	10.48	2.84	10.38	1.60	0.896	0.05
Letter Sequencing	11.43	2.40	10.23	1.90	0.070	0.57
Number-Letter Sequencing	11.29	1.42	9.15	2.43	0.001*	1.07
Motor Speed	11.48	1.44	11.15	2.05	0.531	0.19
D-KEFS Verbal Fluency Test						
Letter Fluency	11.14	2.97	9.12	2.88	0.023*	0.71
Category Fluency	12.14	3.07	10.81	2.71	0.126	0.47
Category Switching	11.86	2.35	10.65	3.22	0.147	0.43
WAIS						
Symbol Search	11.52	4.32	10.88	2.50	0.552	0.19
Digit Symbol Coding	10.62	2.62	8.65	2.40	0.011*	0.81
Processing Speed Index	105.67	16.56	98.50	11.64	0.103	0.52

Group differences on the measures reported in the table were tested using independent *t* tests.

Neuropsychological analysis used scaled scores. The WAIS Processing Speed Index is the sum of the scaled scores of Symbol Search and Digit Symbol Coding to create a composite score.

*Statistically significant ($p < 0.05$).

mTBI, mild traumatic brain injury; D-KEFS, Kaplan Executive Function System; WAIS, Wechsler Adult Intelligence Scale.

Making Test has a visual scanning condition and then requires participants to connect circles as quickly as possible in numerical, alphabetical, and alternating numerical/alphabetical orders. The scaled score for the latter condition was used in analyses as a measure of cognitive flexibility in visual-motor sequencing. The D-KEFS Verbal Fluency Test requires participants to generate words as quickly as possible beginning with particular letters (Letter Fluency), in specified semantic categories (Category Fluency), and while shifting between semantic categories (Category Switching); scaled scores for each condition were used.[60] The Trail Making and Verbal Fluency tests are sensitive to subtle cognitive-shifting deficits relevant to the mTBI population. As for processing speed, the WAIS Symbol Search subtest requires a participant to scan a target group and search a group of symbols, indicating whether one of the target symbols appears in the search group. In the WAIS Digit Symbol Coding subtest, the participant fills in boxes below digits with symbols that are paired with them in a key at the top of the page. Both of these subtests are timed. Scaled scores from each subtest were combined to create an overall Processing Speed Index. The WAIS III was administered to most participants, although a subset of participants completed the WAIS IV version. Sensitivity analyses were performed removing the WAIS IV and the tests for group differences were unchanged.

The abovementioned neuropsychological tests were embedded within a larger test battery, administered by trained research associates. All tests were performed in a single session, within one week of the MEG/MRI session. One participant was excluded from analyses of the neuropsychological data because of potentially invalid data as indicated by the Test of Memory Malingering. All scores utilized were age-corrected scaled scores based on normative data provided by the test publishers.

MEG data acquisition and signal pre-processing to remove artifacts

Resting-state MEG data were collected using the VectorView™ whole-head MEG system (Elekta-Neuromag, Helsinki, Finland) with 306 MEG channels (see Fig. 1A). Participants were seated in an upright position inside a multi-layer magnetically-shielded room (IMEDCO-AG)[63] at the University of California at San Diego (UCSD) MEG Center. For each subject, two 5 min sessions with eyes closed were acquired. The subjects were instructed to empty their minds and to avoid moving their eyes. Data were sampled at 1000 Hz and were run through a high-pass filter with a 0.1 Hz cutoff, and a low-pass filter with a 330 Hz cutoff. Eye blinks and eye movements were monitored using two pairs of bipolar electrodes with one pair placed above and below the left eye, and the other pair placed on the two temples. The heart signals were monitored with another pair of bipolar electrodes. Precautions were taken to ensure head stability; foam wedges were inserted between the subject's head and the inside of the unit, and a Velcro strap was placed under the subject's chin and anchored in the superior and posterior axes. Head movement across different sessions was about 2–3 mm on average.

To help ensure that participants were alert during the MEG recordings, prior to all of the study sessions they completed a questionnaire about the number of hours they had slept the previous night, how rested they felt, and if there was any reason that they might not be attentive and perform to the best of their abilities (because of headache, pain for example). Participants were scheduled early in the day to avoid fatigue from performing daily activities. In addition, eyes-closed sessions were alternated with eyes-open sessions to monitor online the amount of eye blinking and eye movement. The number of alpha band oscillations, which is consistently associated with tonic alertness, was also monitored online to gauge the cognitive state of subjects. Participants were viewed on a camera, which also allowed for monitoring alertness of each subject.

MEG eyes-closed data were first run through MaxFilter, also known as signal space separation,[64–66] to remove external interferences (e.g., magnetic artifacts caused by metal objects, strong cardiac signals, environment noises). Next, residual artifacts near the sensor array caused by eye movements and residual cardiac signals were removed using independent component analysis using Fast-ICA (http://research.ics.aalto.fi/ica/fastica/).[67,68] The waveforms associated with top independent components (ICs) were examined by an experienced MEG data analyst, along with electrocardiogram (ECG) and electrooculogram (EOG) signals. ICs associated with eye blinks, eye movements, heartbeats, and other artifacts were removed. MEG data during the eyes-open sessions were not used in the present study because of large eye-blink artifacts even after the pre-processing using MaxFilter and Fast-ICA.

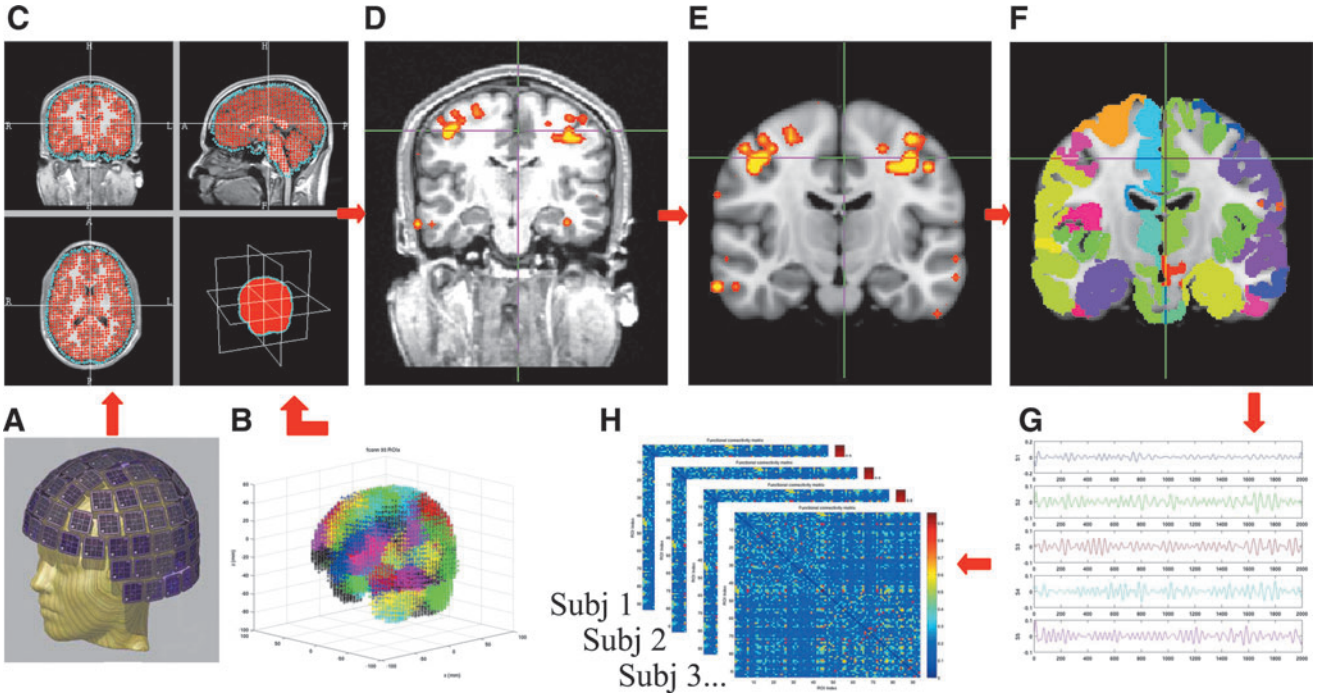

FIG. 1. Schematic flow chart of the resting-state magnetoencephalography (rs-MEG) data analysis. **(A)** MEG sensor measurement. **(B)** Fast vector-based spatio-temporal analysis using an L1-minimum-norm (fast-VESTAL) source grid. **(C)** MRI views of the source grid (red dots) and Boundary Element Method (BEM) mesh (cyan dots). **(D)** High-resolution MEG source image obtained from fast-VESTAL. **(E)** Source image registered to the MNI-152 atlas. **(F)** Activities were grouped into 94 cortical and subcortical gray matter (GM) areas (e.g., regions of interest [ROIs]). **(G)** Examples of ROI source time courses. **(H)** ROI-based functional connectivity (FC) matrix was calculated from each subject. Finally, the mean values across rows (or columns) of the connectivity matrix were used as the connectivity measure from each ROI to the remaining ROIs (i.e., ROI-global FC measure).

Structural MRI, MEG-MRI registration, Boundary Element Method (BEM) forward calculation

A structural MRI of the subject's head was collected using a General Electric 1.5T Excite MRI scanner. The acquisition contains a standard high-resolution anatomical volume with a resolution of $0.94 \times 0.94 \times 1.2\,mm^3$ using a T1-weighted 3D-IR-FSPGR pulse sequence. Scanner-related imaging distortions were corrected using a gradient non-linearity correction approach developed by Dale's laboratory.[69] To co-register the MEG with MRI coordinate systems, three anatomical landmarks (i.e., left and right pre-auricular points, and nasion) were measured for each subject using the Probe Position Identification system (Polhemus, USA). By identifying the same three points on the subject's MR images using MRILAB (Elekta/Neuromag), a transformation matrix involving both rotation and translation between the MEG and MR coordinate systems was generated. To increase the reliability of the MEG-MR co-registration, ~ 80 points on the scalp were digitized with the Polhemus system, in addition to the three landmarks, and those points were co-registered onto the scalp surface of the MR images. The T1-weighted images were also used to extract the brain volume and innermost skull surface (SEGLAB software developed by Elekta/Neuromag). A realistic BEM head model was used for MEG forward calculation.[70,71] The BEM mesh was constructed by tessellating the inner skull surface from the T1-weighted MRI into ~ 6000 triangular elements with ~ 5 mm size. A cubic source grid with a 5 mm size covering cortical and subcortical GM areas based on FCONN brain parcellation[72] was created. Such a source grid was used for calculating the MEG gain (i.e., lead-field) matrix, which leads to a grid with $\sim 10{,}000$ nodes covering the whole brain. The nodes of the source grid were grouped into 94 GM regions (Fig. 1B). Then, the source grid was combined with the BEM mesh in the MRI coordinate (Fig. 1C) for the BEM forward calculation.

Other conventional MRI sequences typical for identifying structural lesions in TBI participants were also performed: 1) axial T2*-weighted; 2) axial fast spin-echo T2-weighted; and 3) axial fluid-attenuated inversion recovery (FLAIR). These conventional MRIs were carefully reviewed by a board-certified neuroradiologist (R.R. Lee) to determine if the subject had visible lesions on MRI.

MEG source magnitude imaging using fast vector-based spatio-temporal analysis using an L1-minimum-norm (fast-VESTAL)

In both 5 min rs-MEG data sessions with eyes closed, sensor waveforms were run through band-pass filters for different frequency bands: alpha band (8–12 Hz), beta band (15–30 Hz), gamma band (30–80 Hz), and low-frequency band (1–7 Hz, delta + theta). The data set was then divided into 4 sec duration epochs, and sensor-waveform covariance matrices were calculated for each epoch. For each frequency band, a total sensor-waveform covariance matrix for the entire 10 min recording was calculated by concatenating the covariance matrices from individual epochs. Using the total covariance matrix, voxelwise MEG slow-wave source magnitude images that covered the whole brain were obtained for each subject following the fast-VESTAL procedure.[73] An objective pre-whitening method was applied to remove correlated environmental noise and objectively select the dominant eigenmodes of sensor-waveform covariance matrix.[73]

The fast-VESTAL technique consists of two steps. First, spatio-temporal L1-minimum-norm MEG source images were obtained for the dominant spatial (i.e., eigen-) modes of sensor-waveform

covariance matrix. Next, accurate source time courses were obtained using an inverse operator constructed from the spatial source images of step 1. This approach has been successfully used to obtain comprehensive MEG source-magnitude images covering the entire brain for different frequency bands of resting-state brain rhythms.[73] The only improvement we made was to adopt a second-order cone programming (SOCP) approach in the minimum L1-norm solver using the SeDuMi software (http://sedumi.ie.lehigh.edu/). SOCP will correct orientation bias in a one-step approach[74,75] instead of our previous two-step approach.[73] The technical details of SOCP Fast-VESTAL formulation is in the appendix of our recent article.[76]

Figure 1D shows an example of high resolution voxelwise source magnitude images (beta band) obtained from fast-VESTAL in a typical participant's native MRI coordinate. The voxelwise source time-courses were also obtained using Fast-VESTAL.[73] The source images were then transformed to the MNI-152[77] Atlas coordinate (Fig. 1E) using a linear affine transformation program, FLIRT, in the FSL software package.[78,79] Next, source activities were grouped into 94 GM ROIs with similar sizes using the FCONN parcellation.[72] In each ROI, an ROI time course was obtained by combining all voxelwise source time courses via singular value decomposition (SVD). The time-domain singular vector associated with the largest singular value was assigned as the ROI-based time source. Figure 1G shows examples of such ROI time courses in beta band. These ROI time courses were used to calculate FC (see next section).

ROI-global FC using ROI source time courses

In each frequency band, two FC measures were examined: 1) lagged cross-correlation (Xcorr), and 2) phase-locking statistics or phase-locking synchrony (PLS).[80] These FC measures focus on different aspects of the temporal characteristics of the MEG signals (see subsequent description). One secondary aim of the present study was to investigate if these different FC measures led to similar or different results.

In the Xcorr approach, for each frequency band, the time course of a 4 sec epoch from one ROI was cross-correlated with the time course in each of the remaining ROIs in the FCONN atlas with time lags. In contrast to conventional correlation analyses, the Xcorr value varies with the time lag variable. Xcorr effectively takes into account the potential time lags between two functional connected brain regions as a result of neuronal signal propagation. We calculated the maximum absolute value of the Xcorr for the −20 ms to +20 ms time lagging window using MATLAB (MathWorks, MA, USA), which resulted in an epoch-wise time-lagged Xcorr value between 0 and 1. The neuronal activity between two ROIs was considered to be completely correlated for Xcorr of 1 and uncorrelated for Xcorr of 0. Next, this step was repeated for all epochs, and the mean value of the lagged cross-correlations was obtained across all epochs, as the ROI lagged cross-correlations. Among all ROIs, this approach resulted in a connectivity matrix for each subject and each frequency band as shown in Figure 1H. We then took the mean value across all rows in the connectivity matrix (excluding the self-connectivity) to form a ROI-global (i.e., whole-brain) connectivity vector with 94 elements. Each element in this vector represented the FC measure from one ROI to all the remaining ROIs. The above-described procedure was performed for all subjects and all four frequency bands listed previously.

In the PLS approach, we adopted the phase-locking values (PLV) measures for frequency-specific synchronization (i.e., transient phase-locking) between two ROI time course signals. PLS measures the significance of the phase covariance between two signals with a reasonable time resolution. The neuronal activity between the two ROIs was considered to be completely synchronized for PLV of 1 and unsynchronized for PLV of 0. Unlike the more traditional method of spectral coherence, PLS separates the phase and amplitude components and can be directly interpreted in the framework of neural integration.[80] In the present study, the frequency increments used in the Morlet wavelet transformation were at 0.5 Hz for the low-frequency band (1–7 Hz) and alpha band (8–12 Hz), at 1 Hz for the beta band (15–30 Hz), and at 2 Hz for the gamma band (30–80 Hz). Similar to the Xcorr approach, ROI-global FC measures were obtained using the PLS approach as the ROI-global connectivity vector with 94 elements.

Statistical analysis

Statistical analyses were performed to assess the group differences for the MEG-based ROI-global FC measures. For each frequency band, Fisher's Z transformation (FZ) was performed on ROI-global FC coefficients. Then, two tailed t tests were used to examine the group differences of the ROI-global FZ coefficients between the blast mTBI and healthy control groups. Familywise error for sets of group tests within each frequency band was corrected using the false discovery rate approach (FDR).

We also tested if abnormal rs-MEG FC in the blast mTBI group correlated with neuropsychological performance. For ROIs that showed significant group differences, Pearson correlations were performed in the blast mTBI group for the ROI-global FZ connectivity coefficients and neuropsychological subtest scores that differed significantly between groups. Scaled scores, which have a normative mean of 10 and an SD of 3, were used in analyses. The familywise error rates for the correlation analyses were FDR adjusted.

Results

Neuropsychological test performance

Table 2 shows the mean (SD) performances for each group on the neuropsychological tests. The mTBI group performed significantly worse than the control group on three of the measures, namely the Number-Letter Sequencing subtest of the Trail Making Test (scaled score), $t(41.371) = 3.753$, $p = 0.001$; Letter Fluency (scaled score), $t(42.324) = 2.360$, $p = 0.023$; and Digit Symbol Coding (scaled score), $t(41.187) = 2.656$, $p = 0.011$.

MEG FC

Figure 2 and Table 3 display abnormal ROI-global FC in blast mTBI participants, compared with military healthy controls, for each frequency band. A high degree of consistency was seen in the tests for group differences using Xcorr and PLS.

For the beta band, both Xcorr and PLS showed increased FC in mTBI participants in 1) right hemisphere memory areas (i.e., parahippocampal gyrus and hippocampus) and an emotion processing center (right amygdala); 2) medial frontal cortex (right vmPFC, rACC, and medial orbital frontal cortex [mOFC]); and 3) left ventrolateral prefrontal cortex (vlPFC). Both measures also showed decreased FC in mTBI in the right frontal pole. However, Xcorr, but not PLS, also detected decreased FC in the right posterior cingulate cortex (PCC) and right supplementary motor area (SMA) of mTBI participants. In contrast, PLS, but not Xcorr, detected increased FC in right posterior parietal lobule and left anterior insular cortices of mTBI participants.

For the gamma band, both Xcorr and PLS showed increased FC in left cerebellum (Crus I) of mTBI participants. In addition, Xcorr, but not PLS, revealed increased FC in right cerebellum of mTBI participants (Crus I).

For the low-frequency band, both Xcorr and PLS showed increased FC in mTBI in: 1) the right putamen, 2) the left hemisphere memory areas (i.e., parahippocampal gyrus and hippocampus),

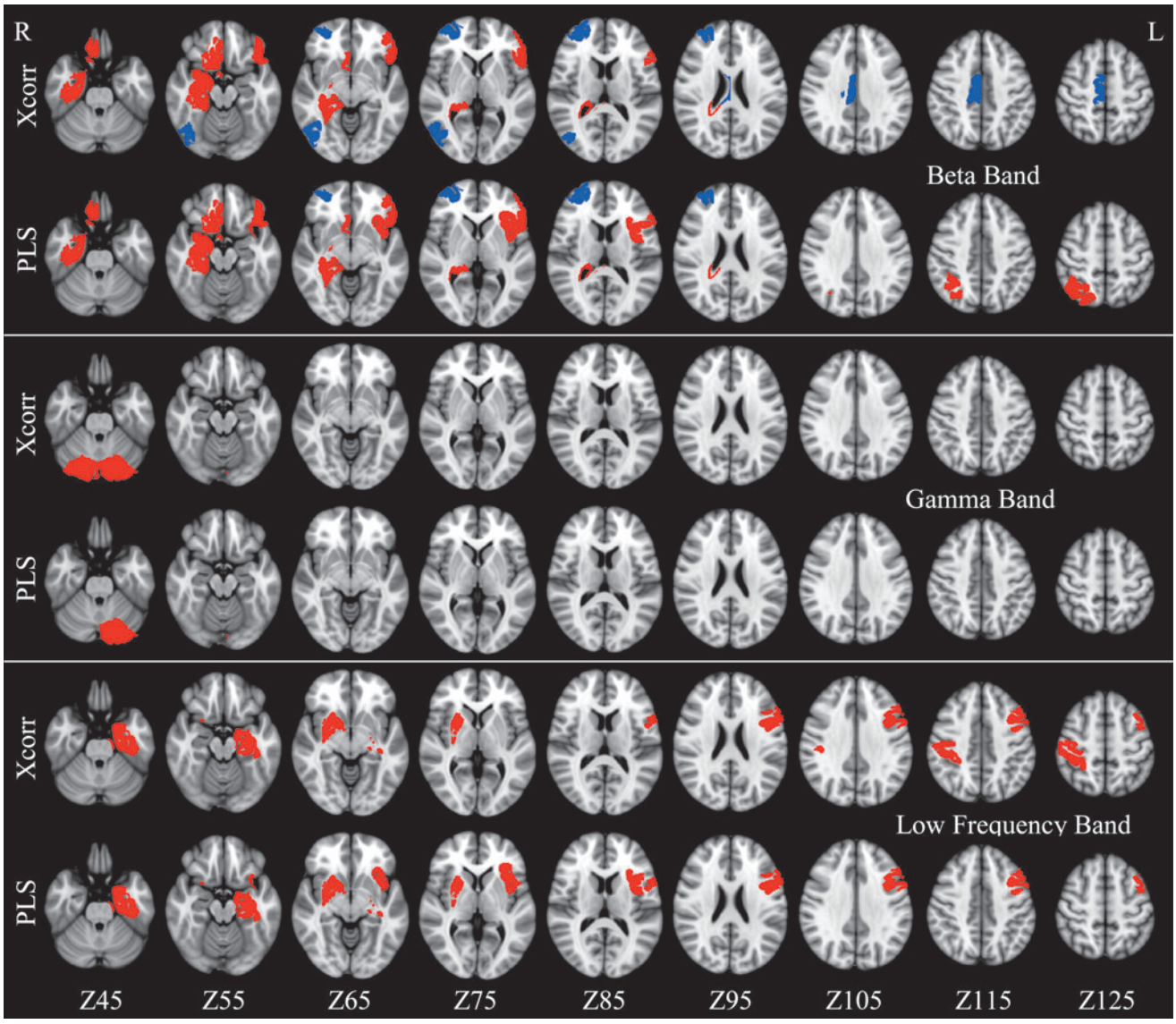

FIG. 2. Abnormal resting-state magnetoencephalography (rs-MEG) functional connectivity (FC) in mild traumatic brain injury (mTBI) participants, compared with healthy control subjects. Red represents significant increases (correct $p < 0.05$), whereas blue represents significant decreases in FC. Top two rows: beta band (15–30 Hz). Middle two rows: gamma band (30–80 Hz). Bottom two rows: low-frequency band (1–7 Hz). For each band, the analyses were performed using cross correlation analysis with ±20 ms lag (Xcorr) and phase-locking synchrony (PLS) analysis. The numbers at the bottom for each axial view are the Z coordinates in MNI-152 atlas.

and an emotion processing hub (right amygdala), and 3) the left dorsolateral prefrontal cortex (dlPFC). Xcorr, but not PLS, also detected increased FC in the right post-central gyrus in mTBI, whereas PLS, but not Xcorr, detected increased FC in the left anterior insular cortex of mTBI participants. Group differences in FC were not significant for the alpha band.

Correlation between abnormal FC and neuropsychological performance

In the blast mTBI group, we examined whether abnormal FC measures correlated with performance (scaled scores) on neuropsychological measures for which there were group differences (Table 2). Scatter plots of significant correlations are displayed in Figure 3. FC of the left vlPFC (PLS, beta band) was negatively correlated with Letter Fluency scores ($r = -0.50$, correct $p < 0.05$, Fig. 3A) and Number-Letter Sequencing scores on the Trail Making Test ($r = -0.47$, correct $p < 0.05$, Fig. 3B), indicating that aberrantly stronger FC of this region was associated with poorer executive functioning. In contrast, WAIS Digit Symbol Coding scores were positively correlated with FC of the left vlPFC for the beta band using Xcorr ($r = 0.66$, correct $p < 0.01$, Fig. 3C) and using PLS ($r = 0.60$, correct $p < 0.05$, not shown), indicating that aberrantly stronger FC of this region was associated with better processing speed. No significant correlations were found between FC and scores on these tests in the control group.

Post-hoc partial correlation analyses, controlling for age, were conducted to examine the effect of age on the correlations between FC measures and neuropsychological performances. The results remained virtually the same, with the partial correlation values (r_p),

Table 3. Brain Areas Showing Abnormal ROI-Global FC in mTBI for Different Frequency Bands Associated with the Xcorr and PLS Measures

	Beta band		*Gamma band*		*Low-freq band*	
Brain Regions	*Xcorr*	*PLS*	*Xcorr*	*PLS*	*Xcorr*	*PLS*
R parahippocampal gyrus, anterior div.	↑	↑				
R parahippocampal gyrus, posterior div.	↑	↑				
R hippocampus and R amygdala	↑	↑				
R vmPFC, R rACC, and R medial OFC	↑	↑				
R frontal pole	↓	↓				
R putamen					↑	↑
R post-central gyrus					↑	
R PCC and R SMA	↓					
R superior parietal lobule		↑				
R inferior-lateral occipital cortex	↓					
R cerebellum (Crus I)			↑			
L parahippocampal gyrus, anterior div.					↑	↑
L hippocampus and R amygdala					↑	↑
L vlPFC	↑	↑				
L dlPFC					↑	↑
L anterior insular cortex		↑				↑
L cerebellum (Crus I)			↑	↑		

Up arrows designate increased FC, whereas down arrows designate decreased FC in blast the blast mTBI group relative to the control group.

ROI, region of interest; FC, functional connectivity; mTBI, mild traumatic brain injury; Xcorr, lagged cross-correlation; PLS, phase-locking synchrony; vmPFC ventromedial frontal cortex; rACC, rostral anterior cingulate cortex; OFC, orbital frontal cortex; PCC, posterior cingulate cortex; SMA, supplementary motor area; vlPFC, ventrolateral prefrontal cortex; dlPFC, dorsolateral prefrontal cortex

after controlling for age, being within 4% the original correlation values (i.e., $[r\text{-}r_p]/r < 0.04$). Gender had no effect on the result, because all participants were male.

Discussion

In the present study, aberrant functional connectivity in blast mTBI was analyzed for the first time using rs-MEG source imaging. In comparison with a well-matched military control group, the blast mTBI group was predominantly characterized by increased ROI-global FC in the: 1) prefrontal cortex (vmPFC, rACC, vlPFC, and dlPFC); 2) medial temporal lobe (bilateral parahippocampus, hippocampus, and amygdala); and 3) putamen and cerebellum (Crus I). An exception was the right frontal pole for which FC was decreased in blast mTBI. These group differences were found for both Xcorr and PLS measures of FC, suggesting that disturbances in global FC of these regions in blast mTBI are reliable. A novel finding was that abnormal FC in blast mTBI was found mainly in the beta and low-frequency bands, with some in the gamma band; however, alpha-band intrinsic FC was preserved. Moreover, aberrant increases in the FC of the left vlPFC in blast mTBI participants were associated with poorer executive functioning, but better processing speed. Altogether, these results suggest that multiple mechanisms may alter ROI-global FC in blast mTBI, and some disturbances are associated with the cognitive sequelae of the injury.

Abnormal increases in FC in blast mTBI

FC in the blast mTBI group was mostly increased relative to the control group, consistent with similar findings from rs-fMRI studies of non-blast-related mTBI. For example, our finding of increased FC of the cerebellum (Xcorr and PLS) and anterior insular cortex (PLS) is consistent with findings of increased spatial coactivity in mTBI from the same brain areas in a recent rs-fMRI study.[38] In addition, increased FC in the left vlPFC is compatible with an rs-fMRI mTBI study for which FC was increased between the vlPFC and rACC.[40] Our findings build on past results, showing for the first time that different frequency bands are associated with abnormal increases in FC of the prefrontal cortices (beta and low frequency) and the cerebellum (gamma). In contrast, an rs-MEG study by

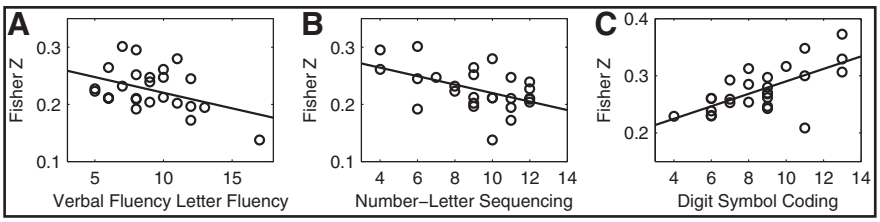

FIG. 3. Functional connectivity (FC) (y-axis) correlated with neuropsychological examinations (x-axis) in blast mild traumatic brain injury (mTBI) group. **(A)** FC of the left ventrolateral prefrontal cortex (vlPFC) (phase-locking synchrony [PLS], beta band) was negatively correlated with Letter Fluency scores ($r = -0.50$, correct $p < 0.05$). **(B)** FC of the left vlPFC (PLS, beta band) was negatively correlated with Number-Letter Sequencing scores on the Trail Making Test ($r = -0.47$, correct $p < 0.05$). **(C)** FC of the left vlPFC (Xcorr, the beta) was positively correlated with Digit Symbol Coding scores ($r = 0.66$, correct $p < 0.01$).

Tarapore and colleagues reported decreases in region-to-global FC from bilateral vlPFC areas.[50] This discrepancy may be the result of their inclusion of more severe TBI patients, who possibly sustained greater damage to white matter (WM) tracks underlying vlPFC and other GM regions, which could lead to disconnection, and hence, reduced FC.

We also found robust FC increases in the medial temporal lobe (bilateral parahippocampus, hippocampus, and amygdala) in blast mTBI, which has not been reported previously. Although Sours and colleagues reported a nonsignificant trend for increased FC of the parahippocampal gyri in chronic asymptomatic mTBI (rs-fMRI), and suggested that the finding was caused by a compensatory mechanism,[27] the absence of significant group differences may related to the sensitivity of their rs-fMRI approach. Future studies using electromagnetic imaging techniques (e.g., rs-MEG) in chronic asymptomatic mTBI may be needed to further address this issue.

The hippocampus, parahippocampus, and amygdala are key areas of the limbic system involved in memory and decision-making and in linking emotional processing with cognition.[81] A positron emission topography (PET) study demonstrated that these regions are vulnerable to blast mTBI.[82] Abnormal activation of medial temporal regions and the vmPFC is also a characteristic of military service members exposed to blast who developed PTSD.[15,83] Our finding extends these results, demonstrating for the first time that different frequency bands are also associated with FC increases in medial temporal areas (beta and low-frequency bands), suggesting new markers of abnormal brain interactions following blast mTBI.

Associations between aberrantly increased FC and cognition in blast mTBI

It is well known that intrinsic FC partly shapes cognitive control. Indeed, we found that abnormal increases in FC of the left vlPFC in mTBI were associated with better processing efficiency in mTBI participants, but worse performance on tests of executive functioning that contained a language component (Fig. 3). The left vlPFC includes BA 47 and Broca's area (BA 44, 45), which mediates expressive language.[76,81] However, contemporary research demonstrates that the left vlPFC plays a broader role, beyond strict language production, in cognitive control. An influential view maintains that areas of the left vlPFC can be distinguished by their strategic control demands, namely controlled retrieval (BA 47) and post-retrieval selection (BA 44, 45) processes,[84,85] which are vital for flexible behavior. Controlled retrieval activates goal-relevant knowledge in a top-down manner, such as required for Letter Fluency. In contrast, post-retrieval selection processes resolve competition among simultaneously competing representations during working memory and task switching, as required for Letter-Number Sequencing. Although this task largely probes for visual attention and psychomotor speed, vlPFC mediation of performance is suggested by the associated between greater bilateral BA 44 activation and higher accuracy on a modified version of this task.[86] Moreover, faster rates of performance on digit-symbol tasks are associated with greater FC of frontal-parietal and frontal-occipital networks, which include the vlPFC.[87] Altogether, this result may indicate that vlPFC disinhibition facilitates communications with remote structures that support visual scanning and psychomotor speed. This interpretation also comports with our finding that aberrant vlPFC FC was confined to the beta band, which is linked to communications requiring long-range or inter-regional networks.[88,89]

At the same time, disruptions in the intrinsic FC of a brain region may have disparate effects on the performances of different tasks, because of the dynamic reconfiguration of cognitive-control networks, wherein cooperation and competition within and outside networks change in a context-dependent manner.[90–92] Another consideration is that compensation after brain injury, as signified by increased FC (see subsequent discussion), may be more effective under lower than under higher information processing demands, as it is in normal aging, mild cognitive impairment, and Parkinson's disease.[93,94] This is compatible with our finding that stronger vlPFC FC was associated with better processing speed, yet poorer executive functioning.

Abnormal decrease in FC of the frontal pole in blast mTBI

Despite our finding of mainly increased FC throughout the brain, decreased FC of the right frontal pole was observed in the blast mTBI group. Abnormal FC of the frontal pole in mTBI has not been previously reported in rs-fMRI or rs-MEG studies. However, the frontal pole is known to connect with the other parts of the brain through several WM tracts including forceps minor (FM), inferior frontal-occipital fasciculus (IFOF), uncinate fasciculus (UF), and superior longitudinal fasciculus (SLF).[95] Diffusion tensor imaging (DTI) studies have shown reduced fractional anisotropy (FA) in the IFOF and the FM[96] in a mixed group of mild to severe TBI patients. FA in the UF is also reduced in patients with mTBI.[97] We suggest that the disruption of WM tracts could affect communication of the frontal pole with the other parts of the brain, which may result in reduced FC. Although relationships between FC of the frontal pole and cognitive measures were not found, our neuropsychological tests did not probe for higher-level cognitive processes (e.g., planning, integrating concurrent mental plans, problem solving) classically associated with more anterior regions of the PFC.[98–100]

Increased and decreased FC suggesting different mechanisms in mTBI

Generally speaking, our findings of increased and decreased FCs in blast mTBI are consistent with previous rs-fMRI[33–41] and rs-MEG studies,[52–54] and suggest that multiple mechanisms may underlie different patterns of aberrant intrinsic FC in individuals with mTBI. A leading model of TBI, the diffuse axonal injury (DAI) model, maintains that injury in WM tracts is a major contributor to the PCS and cognitive deficits in mTBI patients.[101] DAI is commonly induced by sudden acceleration-deceleration or by rotational forces. One expected consequence of DAI in WM is the disruption of neuronal communication among GM areas, which may lead to decreased FC with other brain regions, especially if axonal damage is substantial. For example, reduced FC is consistently found in patients with Alzheimer's disease and schizophrenia,[102–106] wherein structural changes in WM tissue are also found.[107–112] Therefore, the DAI model can explain the abnormally decreased FC in the right frontal pole in the present study. However, the DAI model has difficulties explaining the largely increased FC found in the present study and similar findings in other rs-fMRI and rs-MEG studies.

A neurobiological model of TBI is the glutamate-based over-excitation and GABAergic disinhibition injury model, which emphasizes injuries in GM neurons.[113–116] According to this model, injury to the brain causes glutamate excitotoxicity in pyramidal neurons, leading to injury and death of GABAergic interneurons. The dysfunctional GABAergic interneurons create disinhibition in

pyramidal neurons, which produces overexcitation. A similar mechanism is posited for post-traumatic epilepsy (see references in the study by Prince and coworkers[117]), for which increased global FC is well established.[118] Therefore, in contrast to the DAI model, the glutamate overexcitation and GABA disinhibition model posits aberrant GABA intra-neuron functioning, which diminishes the inhibitory influence on pyramidal neurons, thereby causing increased firing and facilitation of network connections that are normally inhibited. This process could lead to increases in FC between the injured GM area and other regions of the brain. Although the GABAergic disinhibition model is compatible with abnormally increased FC in the present study and other rs-fMRI and rs-MEG studies, post-traumatic epilepsy and glutamate excitotoxicity usually exist in severe TBI in the acute phase. The impact of this mechanism in chronic mTBI is unclear. As reviewed by Guerriero and colleagues,[113] several magnetic resonance spectroscopy (MRS) studies report reduced GM glutamate/glutamine, and transcranial magnetic stimulation studies suggest excess inhibition in chronic symptomatic mTBI, rather than excitation, which is likely GABA mediated.

A compelling and more parsimonious mechanism for increases in FC is functional reorganization through compensation, neuronal plasticity, or rerouting of functional connections after mTBI.[17,22,27,40] Aberrantly increased FC can be caused by functional reorganization in both injured and uninjured GM areas.[22,40] For example, Bharath and colleagues[41] found that mTBI patients in the first 36 h after injury exhibit hyperconnectivity of the salience and DMN networks; however, over time, the hyperconnectivity spreads, affecting FC in additional networks. This demonstrates that increases in FC can be both time and area dependent, in accord with principles of brain plasticity,[119] because the TBI brain is changing at the cellular level to compensate for functional impairment.[22] Hence, the variability in regional FC patterns among studies may be partially related to differences in time post-injury and the level at which the brain is analyzed (e.g., ROI, subnetworks, frequency band). To facilitate functional reorganization, both reduced inhibition and increased excitation among brain regions are needed; however, reduced inhibition in the functional reorganization model may not be the result of damage or death in GABA interneurons, but rather of plasticity-related disinhibition in the GABA interneurons.

In summary, some aberrant increases in FC may be compatible with damage to inhibitory interneurons in the glutamate overexcitation and GABA disinhibition model, whereas other increases in FC in chronic mTBI are likely related to compensation or rerouting. Importantly, both increased and decreased connectivity in mTBI have also been found for measures of structural connectivity derived from DTI or other diffusion-based MRI techniques (see review in article by Douglas and coworkers[120]). Therefore, both neuronal damage and functional reorganization/compensation mechanisms underlie disturbances in functional and structural connectivity in mTBI. For this reason, caution should be exercised when interpreting the connectivity findings in mTBI. Moreover, future studies of mTBI are needed that directly link abnormalities in various connectivity measures to specific mechanisms.

Differences across frequency bands in abnormal FC

In the present study, group differences in FC were found mainly in the beta and low-frequency bands, although some differences were seen in the gamma band, notably for the cerebellum. However, intrinsic alpha band activity was preserved in mTBI. We believe that the findings are associated with the roles of these frequency bands in subserving different brain functions. Neuronal activity from different frequency bands is thought to reflect different neuronal mechanisms.

Lower frequency theta band (4–7 Hz) signals have been reported in previous electroencephalographic (EEG) studies, although these signals were predominantly found during task activation (e.g., problem solving).[59,121–124] Increased low-frequency brain rhythm power in the delta band (1–4 Hz) has often been seen in individuals with various neurological disorders, including epilepsy and TBI.[44,46–48,125–130]

Thalamocortical interactions are essential for alpha rhythms, and normal alpha band (8–12 Hz) activity is associated with functional inhibition.[131–133] Sours and colleagues (rs-fMRI) reported increased FC between the thalamus and cortical regions involved in primary sensory processing and between the thalamus and the DMN in acute or subacute mTBI.[17] However, we did not find changes in FC of the thalamus, possibly because of the insensitivity of MEG to deep signals from thalamus.

In contrast, activity in the beta band (15–30 Hz) is associated with communication among remote brain structures, whereas gamma band (30–80 Hz) synchrony promotes local computations.[88,89] Probably because of its role in long-range communication, most of the rs-MEG FC studies have focused on the beta band.[50,134,135] Although the gamma band electromagnetic signals are generated locally, non-local brain areas can still show significant FC as measured by coherence related to the gamma band signals. Using combined electrophysiological and fMRI measurements, studies in both human and animals have shown that gamma-band power exhibits spatial coherence over long time scales with the strongest coherence between functionally related areas that are not necessarily local.[136–140] Unlike alpha-band activity, beta and gamma-band activity does not necessarily have to involve the thalamus.

Traditionally, the neuronal networks associated with different frequency bands are studied separately. The discovery of cross-frequency coupling within the same brain regions provides a new approach for studying cross-frequency band FC (see reviews in the article by Hyafil and coworkers[141]). This form of coding has been most clearly demonstrated in the hippocampus in animal studies, where different spatial information is represented in different gamma subcycles of a theta cycle. In addition, animal studies also suggest that this coding scheme coordinates communication among brain regions and is involved in sensory as well as memory processes.[142] We believe that before applying cross-frequency coupling techniques to mTBI, one must address key questions in animal studies, such as whether cross-frequency coupling is a common feature among different brain areas or whether it exists only within specific regions.

Consistency in group differences between different FC Measures

An important finding was that the two different FC measures exhibited a high degree of consistency in the tests for group differences (Fig. 2 and Table 3), which cross-validates our results and bolsters the level of confidence in the findings. The time lag in the Xcorr analysis was chosen to be in the range of ±20 ms, consistent with typical neuronal delay among different brain areas.[59] The lagged Xcorr is sensitive to phase, but not amplitude changes, and it is easy to compute with low computational costs.[143] The PLV of the PLS is another popular FC measure of phase synchrony in MEG

and EEG, which is also insensitive to amplitude changes.[80] However, the computational cost of using PLS is higher than that of using Xcorr, because a series of Morlet wavelet decomposition are required.

Limitations and Conclusions

One limitation of the study was that we relied on self-report of substance use. This could be addressed in future studies by validation using biological measures. In addition, individuals with mTBI without ongoing PCS were not included in the present study. Future studies are needed to elucidate the difference between individuals with symptomatic mTBI and those who recover fully from mTBI. We also did not directly examine the DAI model of mTBI and its relevance to disturbances in FC. This limitation can be addressed in the future by collecting diffusion MRI data and rs-MEG from the same blast mTBI subjects.

In conclusion, using two different types of rs-MEG FC measures, we found predominantly increased ROI-global FC in blast mTBI, primarily in beta, but also in gamma, and low-frequency bands. The abnormal increases in FC were mainly from prefrontal and medial temporal lobe areas. In contrast, decreases in FC of the right frontal pole were also observed in blast mTBI. Tests of group differences were highly consistent for the two different FC measures. Although the decreases in FC may be associated with DAI in WM tracts, some findings of increased FC may be consistent in part with overexcitation and GABAergic disinhibition of injured GM tissue; however, findings of abnormally increased FC are more parsimoniously explained by functional reorganization via compensation or rerouting mechanisms.

Acknowledgments

This work was supported in part by Merit Review Grants from the Department of Veterans Affairs to M.X. Huang (I01-CX000499, MHBA-010-14F, NURC-022-10F, NEUC-044-06S), R.R. Lee, and D.L. Harrington (I01-CX000146), and Naval Medical Research Center's Advanced Medical Development program (Naval Medical Logistics Command Contract #N62645-11-C-4037, for MRS-II (D.G. Baker, M.X. Huang, V.B. Risbrough). We acknowledge the MRS-II administrative core, Anjana Patel, Andrew De La Rosa, and members of the MRS-II Team, including logistic coordinators, clinician-interviewers, and data collection staff. We thank staff at the VA San Diego Healthcare System and the Veterans Medical Research Foundation (VRMF). We also thank the participating Marines and veteran volunteers for their military service and participation in this study.

Author Disclosure Statement

No competing financial interests exist.

References

1. MacGregor, A.J., Dougherty, A.L., and Galarneau, M.R. (2011). Injury-specific correlates of combat-related traumatic brain injury in Operation Iraqi Freedom. J. Head Trauma Rehabil. 26, 312–318.
2. Bigler, E.D. (2008). Neuropsychology and clinical neuroscience of persistent post-concussive syndrome. J. Int. Neuropsychol. Soc. 14, 1–22.
3. Cooper, D.B., Bunner, A.E., Kennedy, J.E., Balldin, V., Tate, D.F., Eapen, B.C., and Jaramillo, C.A. (2015). Treatment of persistent post-concussive symptoms after mild traumatic brain injury: a systematic review of cognitive rehabilitation and behavioral health interventions in military service members and veterans. Brain Imaging Behav. 9, 403–420.
4. Schneiderman, A.I., Braver, E.R., and Kang, H.K. (2008). Understanding sequelae of injury mechanisms and mild traumatic brain injury incurred during the conflicts in Iraq and Afghanistan: persistent postconcussive symptoms and posttraumatic stress disorder. Am. J. Epidemiol. 167, 1446–1452.
5. Terrio, H., Brenner, L.A., Ivins, B.J., Cho, J.M., Helmick, K., Schwab, K., Scally, K., Bretthauer, R., and Warden, D. (2009). Traumatic brain injury screening: preliminary findings in a US Army Brigade Combat Team. J. Head Trauma Rehabil. 24, 14–23.
6. Morissette, S.B., Woodward, M., Kimbrel, N.A., Meyer, E.C., Kruse, M.I., Dolan, S., and Gulliver, S.B. (2011). Deployment-related TBI, persistent postconcussive symptoms, PTSD, and depression in OEF/OIF veterans. Rehabil. Psychol. 56, 340–350.
7. Jeter, C.B., Hergenroeder, G.W., Hylin, M.J., Redell, J.B., Moore, A.N., and Dash, P.K. (2013). Biomarkers for the diagnosis and prognosis of mild traumatic brain injury/concussion. J. Neurotrauma 30, 657–670.
8. Johnston, K.M., Ptito, A., Chankowsky, J., and Chen, J.K. (2001). New frontiers in diagnostic imaging in concussive head injury. Clin. J. Sport Med. 11, 166–175.
9. Kirkwood, M.W., Yeates, K.O., and Wilson, P.E. (2006). Pediatric sport-related concussion: a review of the clinical management of an oft-neglected population. Pediatrics 117, 1359–1371.
10. Bigler, E.D., and Orrison, W.W. (2004). Neuroimaging in sports-related brain injury, in: *Traumatic Brain Injury in Sports: An International Perspective*. M.R. Lovell, R.J. Echemendia, J.T. Barth, and M.W. Collins (eds). Swets and Zeitlinger: Lisse, pps. 71–94.
11. DePalma, R.G., and Hoffman, S.W. (2016). Combat blast related traumatic brain injury (TBI): decade of recognition; promise of progress. Behav. Brain Res. [Epub ahead of print]
12. Young, L., Rule, G.T., Bocchieri, R.T., Walilko, T.J., Burns, J.M., and Ling, G. (2015). When physics meets biology: low and high-velocity penetration, blunt impact, and blast injuries to the brain. Front. Neurol. 6, 89.
13. Young, L.A., Rule, G.T., Bocchieri, R.T., and Burns, J.M. (2015). Biophysical mechanisms of traumatic brain injuries. Semin. Neurol. 35, 5–11.
14. Hoge, C.W., McGurk, D., Thomas, J.L., Cox, A.L., Engel, C.C., and Castro, C.A. (2008). Mild traumatic brain injury in U.S. soldiers returning from Iraq. N. Engl. J. Med. 358, 453–463.
15. Huang, M., Risling, M., and Baker, D.G. (2016). The role of biomarkers and MEG-based imaging markers in the diagnosis of post-traumatic stress disorder and blast-induced mild traumatic brain injury. Psychoneuroendocrinology 63, 398–409.
16. Lee, K.Y., Nyein, M.K., Moore, D.F., Joannopoulos, J.D., Socrate, S., Imholt, T., Radovitzky, R., and Johnson, S.G. (2011). Blast-induced electromagnetic fields in the brain from bone piezoelectricity. Neuroimage 54, Suppl. 1, S30–S36.
17. Sours, C., George, E.O., Zhuo, J., Roys, S., and Gullapalli, R.P. (2015). Hyper-connectivity of the thalamus during early stages following mild traumatic brain injury. Brain Imaging Behav. 9, 550–563.
18. Abbas, K., Shenk, T.E., Poole, V.N., Breedlove, E.L., Leverenz, L.J., Nauman, E.A., Talavage, T.M., and Robinson, M.E. (2015). Alteration of default mode network in high school football athletes due to repetitive subconcussive mild traumatic brain injury: a resting-state functional magnetic resonance imaging study. Brain Connect. 5, 91–101.
19. Sours, C., Zhuo, J., Janowich, J., Aarabi, B., Shanmuganathan, K., and Gullapalli, R.P. (2013). Default mode network interference in mild traumatic brain injury – a pilot resting state study. Brain Res. 1537, 201–215.
20. Shumskaya, E., Andriessen, T.M.J.C., Norris, D.G., and Vos, P.E. (2012). Abnormal whole-brain functional networks in homogeneous acute mild traumatic brain injury. Neurology 79, 175–182.
21. Tang, L., Ge, Y., Sodickson, D.K., Miles, L., Zhou, Y., Reaume, J., and Grossman, R.I. (2011). Thalamic resting-state functional networks: disruption in patients with mild traumatic brain injury. Radiology 260, 831–840.
22. Tang, C.Y., Eaves, E., ms-O'Connor, K., Ho, L., Leung, E., Wong, E., Carpenter, D., Ng, J., Gordon, W., and Pasinetti, G. (2012). Diffuse disconnectivity in TBI: a resting state fMRI and DTI study. Transl. Neurosci. 3, 9–14.
23. Gilmore, C.S., Camchong, J., Davenport, N.D., Nelson, N.W., Kardon, R.H., Lim, K.O., and Sponheim, S.R. (2016). Deficits in visual

system functional connectivity after blast-related mild TBI are associated with injury severity and executive dysfunction. Brain Behav. 6, e00454.
24. Xiong, K.L., Zhang, J.N., Zhang, Y.L., Zhang, Y., Chen, H., and Qiu, M.G. (2016). Brain functional connectivity and cognition in mild traumatic brain injury. Neuroradiology 58, 733–739.
25. van der Horn, H.J., Liemburg, E.J., Scheenen, M.E., de Koning, M.E., Marsman, J.-B.C., Spikman, J.M., and van der Naalt, J. (2016). Brain network dysregulation, emotion, and complaints after mild traumatic brain injury. Hum. Brain Mapp. 37, 1645–1654.
26. Zhan, J., Gao, L., Zhou, F., Kuang, H., Zhao, J., Wang, S., He, L., Zeng, X., and Gong, H. (2015). Decreased regional homogeneity in patients with acute mild traumatic brain injury: a resting-state fmri study. J. Nerv. Ment. Dis. 203, 786–791.
27. Sours, C., Chen, H., Roys, S., Zhuo, J., Varshney, A., and Gullapalli, R.P. (2015). Investigation of multiple frequency ranges using discrete wavelet decomposition of resting-state functional connectivity in mild traumatic brain injury patients. Brain Connect. 5, 442–450.
28. Robinson, M.E., Lindemer, E.R., Fonda, J.R., Milberg, W.P., McGlinchey, R.E., and Salat, D.H. (2015). Close-range blast exposure is associated with altered functional connectivity in Veterans independent of concussion symptoms at time of exposure. Hum. Brain Mapp. 36, 911–922.
29. Sours, C., Rosenberg, J., Kane, R., Roys, S., Zhuo, J., Shanmuganathan, K., and Gullapalli, R.P. (2015). Associations between interhemispheric functional connectivity and the Automated Neuropsychological Assessment Metrics (ANAM) in civilian mild TBI. Brain Imaging Behav. 9, 190–203.
30. Zhou, Y., Lui, Y.W., Zuo, X.-N., Milham, M.P., Reaume, J., Grossman, R.I., and Ge, Y. (2014). Characterization of thalamocortical association using amplitude and connectivity of functional MRI in mild traumatic brain injury. J. Magn. Reson. Imaging 39, 1558–1568.
31. Zhou, Y., Milham, M.P., Lui, Y.W., Miles, L., Reaume, J., Sodickson, D.K., Grossman, R.I., and Ge, Y. (2012). Default-mode network disruption in mild traumatic brain injury. Radiology 265, 882–892.
32. Vakhtin, A.A., Calhoun, V.D., Jung, R.E., Prestopnik, J.L., Taylor, P.A., and Ford, C.C. (2013). Changes in intrinsic functional brain networks following blast-induced mild traumatic brain injury. Brain Inj. 27, 1304–1310.
33. Han, K., Mac Donald, C.L., Johnson, A.M., Barnes, Y., Wierzechowski, L., Zonies, D., Oh, J., Flaherty, S., Fang, R., Raichle, M.E., and Brody, D.L. (2014). Disrupted modular organization of resting-state cortical functional connectivity in U.S. military personnel following concussive ''mild'' blast-related traumatic brain injury. Neuroimage. 84, 76–96.
34. Iraji, A., Chen, H., Wiseman, N., Zhang, T., Welch, R., O'Neil, B., Kulek, A., Ayaz, S.I., Wang, X., Zuk, C., Haacke, E.M., Liu, T., and Kou, Z. (2016). Connectome-scale assessment of structural and functional connectivity in mild traumatic brain injury at the acute stage. NeuroImage Clin. 12, 100–115.
35. Banks, S.D., Coronado, R.A., Clemons, L.R., Abraham, C.M., Pruthi, S., Conrad, B.N., Morgan, V.L., Guillamondegui, O.D., and Archer, K.R. (2016). Thalamic functional connectivity in mild traumatic brain injury: longitudinal associations with patient-reported outcomes and neuropsychological tests. Arch. Phys. Med. Rehabil. 97, 1254–1261.
36. Sours, C., Zhuo, J., Roys, S., Shanmuganathan, K., and Gullapalli, R.P. (2015). Disruptions in resting state functional connectivity and cerebral blood flow in mild traumatic brain injury patients. PloS One 10, e0134019.
37. Iraji, A., Benson, R.R., Welch, R.D., O'Neil, B.J., Woodard, J.L., Ayaz, S.I., Kulek, A., Mika, V., Medado, P., Soltanian-Zadeh, H., Liu, T., Haacke, E.M., and Kou, Z. (2015). Resting state functional connectivity in mild traumatic brain injury at the acute stage: independent component and seed-based analyses. J. Neurotrauma 32, 1031–1045.
38. Nathan, D.E., Oakes, T.R., Yeh, P.H., French, L.M., Harper, J.F., Liu, W., Wolfowitz, R.D., Wang, B.Q., Graner, J.L., and Riedy, G. (2015). Exploring variations in functional connectivity of the resting state default mode network in mild traumatic brain injury. Brain Connect. 5, 102–114.
39. Johnson, B., Zhang, K., Gay, M., Horovitz, S., Hallett, M., Sebastianelli, W., and Slobounov, S. (2012). Alteration of brain default network in subacute phase of injury in concussed individuals: resting-state fMRI study. NeuroImage 59, 511–518.
40. Mayer, A.R., Mannell, M.V., Ling, J., Gasparovic, C., and Yeo, R.A. (2011). Functional connectivity in mild traumatic brain injury. Hum. Brain Mapp. 32, 1825–1835.
41. Bharath, R.D., Munivenkatappa, A., Gohel, S., Panda, R., Saini, J., Rajeswaran, J., Shukla, D., Bhagavatula, I.D., and Biswal, B.B. (2015). Recovery of resting brain connectivity ensuing mild traumatic brain injury. Front. Hum. Neurosci. 9, 513.
42. Eklund, A., Nichols, T.E., and Knutsson, H. (2016). Cluster failure: why fMRI inferences for spatial extent have inflated false-positive rates. Proc. Natl. Acad. Sci. U. S. A. 113, 7900–7905.
43. Leahy, R.M., Mosher, J.C., Spencer, M.E., Huang, M.X., and Lewine, J.D. (1998). A study of dipole localization accuracy for MEG and EEG using a human skull phantom. Electroencephalogr. Clin. Neurophysiol. 107, 159–173.
44. Lewine, J.D., Davis, J.T., Sloan, J.H., Kodituwakku, P.W., and Orrison, W.W., Jr. (1999). Neuromagnetic assessment of pathophysiologic brain activity induced by minor head trauma. AJNR Am. J. Neuroradiol. 20, 857–866.
45. Lewine, J.D., Davis, J.T., Bigler, E.D., Thoma, R., Hill, D., Funke, M., Sloan, J.H., Hall, S., and Orrison, W.W. (2007). Objective documentation of traumatic brain injury subsequent to mild head trauma: multimodal brain imaging with MEG, SPECT, and MRI. J. Head Trauma Rehabil. 22, 141–155.
46. Huang, M.X., Theilmann, R.J., Robb, A., Angeles, A., Nichols, S., Drake, A., D'Andrea, J., Levy, M., Holland, M., Song, T., Ge, S., Hwang, E., Yoo, K., Cui, L., Baker, D.G., Trauner, D., Coimbra, R., and Lee, R.R. (2009). Integrated imaging approach with MEG and DTI to detect mild traumatic brain injury in military and civilian patients. J. Neurotrauma 26, 1213–1226.
47. Huang, M.-X., Nichols, S., Robb, A., Angeles, A., Drake, A., Holland, M., Asmussen, S., D'Andrea, J., Chun, W., Levy, M., Cui, L., Song, T., Baker, D.G., Hammer, P., McLay, R., Theilmann, R.J., Coimbra, R., Diwakar, M., Boyd, C., Neff, J., Liu, T.T., Webb-Murphy, J., Farinpour, R., Cheung, C., Harrington, D.L., Heister, D., and Lee, R.R. (2012). An automatic MEG low-frequency source imaging approach for detecting injuries in mild and moderate TBI patients with blast and non-blast causes. NeuroImage 61, 1067–1082.
48. Huang, M.-X., Nichols, S., Baker, D.G., Robb, A., Angeles, A., Yurgil, K.A., Drake, A., Levy, M., Song, T., McLay, R., Theilmann, R.J., Diwakar, M., Risbrough, V.B., Ji, Z., Huang, C.W., Chang, D.G., Harrington, D.L., Muzzatti, L., Canive, J.M., Christopher Edgar, J., Chen, Y.-H., and Lee, R.R. (2014). Single-subject-based whole-brain MEG slow-wave imaging approach for detecting abnormality in patients with mild traumatic brain injury. NeuroImage Clin. 5, 109–119.
49. Robb Swan, A., Nichols, S., Drake, A., Angeles, A., Diwakar, M., Song, T., Lee, R.R., and Huang, M.-X. (2015). Magnetoencephalography slow-wave detection in patients with mild traumatic brain injury and ongoing symptoms correlated with long-term neuropsychological outcome. J. Neurotrauma 32, 1510–1521.
50. Tarapore, P.E., Findlay, A.M., Lahue, S.C., Lee, H., Honma, S.M., Mizuiri, D., Luks, T.L., Manley, G.T., Nagarajan, S.S., and Mukherjee, P. (2013). Resting state magnetoencephalography functional connectivity in traumatic brain injury. J. Neurosurg. 118, 1306–1316.
51. Alhourani, A., Wozny, T.A., Krishnaswamy, D., Pathak, S., Walls, S.A., Ghuman, A.S., Krieger, D.N., Okonkwo, D.O., Richardson, R.M., and Niranjan, A. (2016). Magnetoencephalography-based identification of functional connectivity network disruption following mild traumatic brain injury. J. Neurophysiol. 116, 1840–1847.
52. Antonakakis, M., Dimitriadis, S.I., Zervakis, M., Micheloyannis, S., Rezaie, R., Babajani-Feremi, A., Zouridakis, G., and Papanicolaou, A.C. (2016). Altered cross-frequency coupling in resting-state MEG after mild traumatic brain injury. Int. J. Psychophysiol. 102, 1–11.
53. Dimitriadis, S.I., Zouridakis, G., Rezaie, R., Babajani-Feremi, A., and Papanicolaou, A.C. (2015). Functional connectivity changes detected with magnetoencephalography after mild traumatic brain injury. NeuroImage Clin. 9, 519–531.
54. Dunkley, B.T., Da Costa, L., Bethune, A., Jetly, R., Pang, E.W., Taylor, M.J., and Doesburg, S.M. (2015). Low-frequency connectivity is associated with mild traumatic brain injury. NeuroImage Clin. 7, 611–621.

55. The Management of Concussion/mTBI Working Group (2009). VA/DoD clinical practice guideline for management of concussion/mild traumatic brain injury. J. Rehabil. Res. Dev. 46, CP1-68.
56. Teasdale, G., and Jennett, B. (1974). Assessment of coma and impaired consciousness. A practical scale. Lancet 2, 81–84.
57. McLean, A., Jr., Dikmen, S., Temkin, N., Wyler, A.R., and Gale, J.L. (1984). Psychosocial functioning at 1 month after head injury. Neurosurgery 14, 393–399.
58. Dikmen, S.S., Ross, B.L., Machamer, J.E., and Temkin, N.R. (1995). One year psychosocial outcome in head injury. J. Int. Neuropsychol. Soc. 1, 67–77.
59. Niedermeyer, E., and Lopes da Silva, F.H. (2005). *Electroencephalography: Basic Principles, Clinical Applications, and Related Fields.* Lippincott Williams & Wilkins: Philadelphia, Baltimore, New York, London, Buenos Aires, Hong Kong, Sydney, Tokyo.
60. Delis, D.C., Kaplan, E., and Kramer, J.H. (2001). *Delis-Kaplan Executive Function System.* The Psychological Corporation: San Antonio.
61. Wechsler, D. (1997). *WAIS-III Wechsler Adult Intelligence Scale.* The Psychological Corporation: San Antonio.
62. Wechsler, D. (2008). *WAIS-IV Wechsler Adult Intelligence Scale.* The Psychological Corporation: San Antonio.
63. Cohen, D., Schlapfer, U., Ahlfors, S., Hamalainen, M., and Halgren, E. (2002). New six-layer magnetically-shielded room for MEG, in: *Proceedings of the 13th International Conference on Biomagnetism*. H.H.J Nowak, and F. Giebler (eds). VDE Verlag: Jena, pps. 919–921.
64. Taulu, S., Simola, J., and Kajola, M. (2004). MEG recordings of DC fields using the signal space separation method (SSS). Neurol. Clin. Neurophysiol. 2004, 35.
65. Taulu, S., Kajola, M., and Simola, J. (2004). Suppression of interference and artifacts by the signal space separation method. Brain Topogr. 16, 269–275.
66. Song, T., Gaa, K., Cui, L., Feffer, L., Lee, R.R., and Huang, M. (2008). Evaluation of signal space separation via simulation. Med. Biol. Eng. Comput. 46, 923–932.
67. Hyvarinen, A., and Oja, E. (2000). Independent component analysis: algorithms and applications. Neural. Netw. 13, 411–430.
68. Hyvarinen, A. (1999). Fast and robust fixed-point algorithms for independent component analysis. IEEE Trans. Neural Netw. 10, 626–634.
69. Jovicich, J., Czanner, S., Greve, D., Haley, E., van der, K.A., Gollub, R., Kennedy, D., Schmitt, F., Brown, G., Macfall, J., Fischl, B., and Dale, A. (2006). Reliability in multi-site structural MRI studies: effects of gradient non-linearity correction on phantom and human data. Neuroimage 30, 436–443.
70. Mosher, J.C., Leahy, R.M., and Lewis, P.S. (1999). EEG and MEG: forward solutions for inverse methods. IEEE Trans. Biomed. Eng. 46, 245–259.
71. Huang, M.X., Song, T., Hagler, D.J., Jr., Podgorny, I., Jousmaki, V., Cui, L., Gaa, K., Harrington, D.L., Dale, A.M., Lee, R.R., Elman, J., and Halgren, E. (2007). A novel integrated MEG and EEG analysis method for dipolar sources. Neuroimage 37, 731–748.
72. Shen, X., Tokoglu, F., Papademetris, X., and Constable, R.T. (2013). Groupwise whole-brain parcellation from resting-state fMRI data for network node identification. Neuroimage 82, 403–415.
73. Huang, M.-X., Huang, C.W., Robb, A., Angeles, A., Nichols, S.L., Baker, D.G., Song, T., Harrington, D.L., Theilmann, R.J., Srinivasan, R., Heister, D., Diwakar, M., Canive, J.M., Edgar, J.C., Chen, Y.-H., Ji, Z., Shen, M., El-Gabalawy, F., Levy, M., McLay, R., Webb-Murphy, J., Liu, T.T., Drake, A., and Lee, R.R. (2014). MEG source imaging method using fast L1 minimum-norm and its applications to signals with brain noise and human resting-state source amplitude images. NeuroImage 84, 585–604.
74. Ou, W., Golland, P., and Hamalainen, M. (2008). A distributed spatio-temporal EEG/MEG inverse solver. Med. Image Comput. Comput. Assist. Interv. 11, 26–34.
75. Haufe, S., Tomioka, R., Dickhaus, T., Sannelli, C., Blankertz, B., Nolte, G., and Muller, K.R. (2011). Large-scale EEG/MEG source localization with spatial flexibility. Neuroimage 54, 851–859.
76. Huang, C.W., Huang, M.-X., Ji, Z., Swan, A.R., Angeles, A.M., Song, T., Huang, J.W., and Lee, R.R. (2016). High-resolution MEG source imaging approach to accurately localize Broca's area in patients with brain tumor or epilepsy. Clin. Neurophysiol. 127, 2308–2316.
77. Grabner, G., Janke, A.L., Budge, M.M., Smith, D., Pruessner, J., and Collins, D.L. (2006). Symmetric atlasing and model based segmentation: an application to the hippocampus in older adults. Med. Image Comput. Comput. Assist. Interv. 9, 58–66.
78. Smith, S.M., Jenkinson, M., Woolrich, M.W., Beckmann, C.F., Behrens, T.E., Johansen-Berg, H., Bannister, P.R., De, L.M., Drobnjak, I., Flitney, D.E., Niazy, R.K., Saunders, J., Vickers, J., Zhang, Y., De, S.N., Brady, J.M., and Matthews, P.M. (2004). Advances in functional and structural MR image analysis and implementation as FSL. Neuroimage 23 Suppl. 1, S208–S219.
79. Woolrich, M.W., Jbabdi, S., Patenaude, B., Chappell, M., Makni, S., Behrens, T., Beckmann, C., Jenkinson, M., and Smith, S.M. (2009). Bayesian analysis of neuroimaging data in FSL. Neuroimage 45, S173–S186.
80. Lachaux, J.P., Rodriguez, E., Martinerie, J., and Varela, F.J. (1999). Measuring phase synchrony in brain signals. Hum. Brain Mapp. 8, 194–208.
81. Kandel, E.R., Schwartz, J.H., Jessell, T.M., Siegelbaum, S.A., and Hudspeth, A.J. (2013). *Principles of Neural Science*, 5th ed. McGraw-Hill Companies, Inc.: New York.
82. Stocker, R.P., Cieply, M.A., Paul, B., Khan, H., Henry, L., Kontos, A.P., and Germain, A. (2014). Combat-related blast exposure and traumatic brain injury influence brain glucose metabolism during REM sleep in military veterans. Neuroimage 99, 207–214.
83. Huang, M.-X., Yurgil, K.A., Robb, A., Angeles, A., Diwakar, M., Risbrough, V.B., Nichols, S.L., McLay, R., Theilmann, R.J., Song, T., Huang, C.W., Lee, R.R., and Baker, D.G. (2014). Voxel-wise resting-state MEG source magnitude imaging study reveals neurocircuitry abnormality in active-duty service members and veterans with PTSD. NeuroImage Clin. 5, 408–419.
84. Badre, D., and Wagner, A.D. (2007). Left ventrolateral prefrontal cortex and the cognitive control of memory. Neuropsychologia 45, 2883–2901.
85. Koechlin, E., and Jubault, T. (2006). Broca's area and the hierarchical organization of human behavior. Neuron 50, 963–974.
86. Usui, N., Haji, T., Maruyama, M., Katsuyama, N., Uchida, S., Hozawa, A., Omori, K., Tsuji, I., Kawashima, R., and Taira, M. (2009). Cortical areas related to performance of WAIS Digit Symbol Test: a functional imaging study. Neurosci. Lett. 463, 1–5.
87. Forn, C., Ripolles, P., Cruz-Gomez, A.J., Belenguer, A., Gonzalez-Torre, J.A., and Avila, C. (2013). Task-load manipulation in the Symbol Digit Modalities Test: an alternative measure of information processing speed. Brain Cogn. 82, 152–160.
88. Singer, W. (1999). Neuronal synchrony: a versatile code for the definition of relations? Neuron 24, 49–25.
89. Kopell, N., Ermentrout, G.B., Whittington, M.A., and Traub, R.D. (2000). Gamma rhythms and beta rhythms have different synchronization properties. Proc. Natl. Acad. Sci. USA 97, 1867–1872.
90. Cocchi, L., Zalesky, A., Fornito, A., and Mattingley, J.B. (2013). Dynamic cooperation and competition between brain systems during cognitive control. Trends Cogn. Sci. 17, 493–501.
91. Cole, M.W., Reynolds, J.R., Power, J.D., Repovs, G., Anticevic, A., and Braver, T.S. (2013). Multi-task connectivity reveals flexible hubs for adaptive task control. Nat. Neurosci. 16, 1348–1355.
92. Fornito, A., Harrison, B.J., Zalesky, A., and Simons, J.S. (2012). Competitive and cooperative dynamics of large-scale brain functional networks supporting recollection. Proc. Natl. Acad. Sci. U. S. A. 109, 12788–12793.
93. Grady, C. (2012). The cognitive neuroscience of ageing. Nat. Rev. Neurosci. 13, 491–505.
94. Harrington, D.L., Castillo, G.N., Reed, J.D., Song, D.D., Litvan, I., and Lee, R.R. (2014). Dissociation of neural mechanisms for intersensory timing deficits in Parkinson's disease. Timing Amp. Time Percept. 2, 145–168.
95. Orr, J.M., Smolker, H.R., and Banich, M.T. (2015). Organization of the human frontal pole revealed by large-scale DTI-based connectivity: implications for control of behavior. PLoS One 10, e0124797.
96. Kraus, M.F., Susmaras, T., Caughlin, B.P., Walker, C.J., Sweeney, J.A., and Little, D.M. (2007). White matter integrity and cognition in chronic traumatic brain injury: a diffusion tensor imaging study. Brain 130, 2508–2519.
97. Niogi, S.N., Mukherjee, P., Ghajar, J., Johnson, C., Kolster, R.A., Sarkar, R., Lee, H., Meeker, M., Zimmerman, R.D., Manley, G.T., and McCandliss, B.D. (2008). Extent of microstructural white matter injury in postconcussive syndrome correlates with impaired cognitive

reaction time: a 3T diffusion tensor imaging study of mild traumatic brain injury. AJNR Am. J. Neuroradiol. 29, 967–973.
98. Braver, T.S., and Bongiolatti, S.R. (2002). The role of frontopolar cortex in subgoal processing during working memory. Neuroimage 15, 523–536.
99. Badre, D. (2008). Cognitive control, hierarchy, and the rostro-caudal organization of the frontal lobes. Trends Cogn. Sci. 12, 193–200.
100. Koechlin, E., and Hyafil, A. (2007). Anterior prefrontal function and the limits of human decision-making. Science 318, 594–598.
101. Hannawi, Y., and Stevens, R.D. (2016). Mapping the connectome following traumatic brain injury. Curr. Neurol. Neurosci. Rep. 16, 44.
102. Chen, Y., Yan, H., Han, Z., Bi, Y., Chen, H., Liu, J., Wu, M., Wang, Y., and Zhang, Y. (2016). Functional activity and connectivity differences of five resting-state networks in patients with Alzheimer's disease or mild cognitive impairment. Curr. Alzheimer. Res. 13, 234–242.
103. Greicius, M.D., Srivastava, G., Reiss, A.L., and Menon, V. (2004). Default-mode network activity distinguishes Alzheimer's disease from healthy aging: evidence from functional MRI. Proc. Natl. Acad. Sci. U.S.A. 101, 4637–4642.
104. Sorg, C., Riedl, V., Muhlau, M., Calhoun, V.D., Eichele, T., Laer, L., Drzezga, A., Forstl, H., Kurz, A., Zimmer, C., and Wohlschlager, A.M. (2007). Selective changes of resting-state networks in individuals at risk for Alzheimer's disease. Proc. Natl. Acad. Sci. U.S.A. 104, 18,760–18,765.
105. Schilbach, L., Hoffstaedter, F., Muller, V., Cieslik, E.C., Goya-Maldonado, R., Trost, S., Sorg, C., Riedl, V., Jardri, R., Sommer, I., Kogler, L., Derntl, B., Gruber, O., and Eickhoff, S.B. (2016). Transdiagnostic commonalities and differences in resting state functional connectivity of the default mode network in schizophrenia and major depression. Neuroimage Clin. 10, 326–335.
106. Liang, M., Zhou, Y., Jiang, T., Liu, Z., Tian, L., Liu, H., and Hao, Y. (2006). Widespread functional disconnectivity in schizophrenia with resting-state functional magnetic resonance imaging. Neuroreport 17, 209–213.
107. Kantarci, K. (2014). Fractional anisotropy of the fornix and hippocampal atrophy in Alzheimer's disease. Front. Aging Neurosci. 6, 316.
108. Douaud, G., Menke, R.A., Gass, A., Monsch, A.U., Rao, A., Whitcher, B., Zamboni, G., Matthews, P.M., Sollberger, M., and Smith, S. (2013). Brain microstructure reveals early abnormalities more than two years prior to clinical progression from mild cognitive impairment to Alzheimer's disease. J. Neurosci. 33, 2147–2155.
109. Mielke, M.M., Okonkwo, O.C., Oishi, K., Mori, S., Tighe, S., Miller, M.I., Ceritoglu, C., Brown, T., Albert, M., and Lyketsos, C.G. (2012). Fornix integrity and hippocampal volume predict memory decline and progression to Alzheimer's disease. Alzheimers Dement. 8, 105–113.
110. Tamnes, C.K., and Agartz, I. (2016). White matter microstructure in early-onset schizophrenia: a systematic review of diffusion tensor imaging studies. J. Am. Acad. Child Adolesc. Psychiatry 55, 269–279.
111. Ellison-Wright, I., and Bullmore, E. (2009). Meta-analysis of diffusion tensor imaging studies in schizophrenia. Schizophr. Res. 108, 3–10.
112. Fitzsimmons, J., Kubicki, M., and Shenton, M.E. (2013). Review of functional and anatomical brain connectivity findings in schizophrenia. Curr. Opin. Psychiatry 26, 172–187.
113. Guerriero, R.M., Giza, C.C., and Rotenberg, A. (2015). Glutamate and GABA imbalance following traumatic brain injury. Curr. Neurol. Neurosci. Rep. 15, 27.
114. Cantu, D., Walker, K., Andresen, L., Taylor-Weiner, A., Hampton, D., Tesco, G., and Dulla, C.G. (2015). Traumatic brain injury increases cortical glutamate network activity by compromising GABAergic control. Cereb. Cortex 25, 2306–2320.
115. Almeida-Suhett, C.P., Prager, E.M., Pidoplichko, V., Figueiredo, T.H., Marini, A.M., Li, Z., Eiden, L.E., and Braga, M.F. (2014). Reduced GABAergic inhibition in the basolateral amygdala and the development of anxiety-like behaviors after mild traumatic brain injury. PLoS One 9, e102627.
116. Giza, C.C., and Hovda, D.A. (2014). The new neurometabolic cascade of concussion. Neurosurgery 75, Suppl. 4, S24–S33.
117. Prince, D.A., Parada, I., Scalise, K., Graber, K., Jin, X., and Shen, F. (2009). Epilepsy following cortical injury: cellular and molecular mechanisms as targets for potential prophylaxis. Epilepsia 50, Suppl. 2, 30–40.
118. Song, J., Nair, V.A., Gaggl, W., and Prabhakaran, V. (2015). Disrupted brain functional organization in epilepsy revealed by graph theory analysis. Brain Connect. 5, 276–283.
119. Kolb, B., and Muhammad, A. (2014). Harnessing the power of neuroplasticity for intervention. Front. Hum. Neurosci. 8, 377.
120. Douglas, D.B., Iv, M., Douglas, P.K., Anderson, A., Vos, S.B., Bammer, R., Zeineh, M., and Wintermark, M. (2015). Diffusion tensor imaging of TBI: potentials and challenges. Top. Magn. Reson. Imaging 24, 241–251.
121. Takahashi, N., Shinomiya, S., Mori, D., and Tachibana, S. (1997). Frontal midline theta rhythm in young healthy adults. Clin. Electroencephalogr. 28, 49–54.
122. Mizuki, Y., Kajimura, N., Kai, S., Suetsugi, M., Ushijima, I., and Yamada, M. (1992). Differential responses to mental stress in high and low anxious normal humans assessed by frontal midline theta activity. Int. J. Psychophysiol. 12, 169–178.
123. Mizuki, Y., Tanaka, M., Isozaki, H., Nishijima, H., and Inanaga, K. (1980). Periodic appearance of theta rhythm in the frontal midline area during performance of a mental task. Electroencephalogr. Clin. Neurophysiol. 49, 345–351.
124. Mizuki, Y., Kajimura, N., Nishikori, S., Imaizumi, J., and Yamada, M. (1984). Appearance of frontal midline theta rhythm and personality traits. Folia. Psychiatr. Neurol. Jpn. 38, 451–458.
125. Baayen, J.C., de, J.A., Stam, C.J., De Munck, J.C., Jonkman, J.J., Trenite, D.G., Berendse, H.W., van Walsum, A.M., Heimans, J.J., Puligheddu, M., Castelijns, J.A., and Vandertop, W.P. (2003). Localization of slow wave activity in patients with tumor-associated epilepsy. Brain Topogr. 16, 85–93.
126. Decker, D.A., Jr., and Knott, J.R. (1972). The EEG in intrinsic supratentorial brain tumors: a comparative evaluation. Electroencephalogr. Clin. Neurophysiol. 33, 303–310.
127. Nagata, K., Gross, C.E., Kindt, G.W., Geier, J.M., and Adey, G.R. (1985). Topographic electroencephalographic study with power ratio index mapping in patients with malignant brain tumors. Neurosurgery 17, 613–619.
128. Vieth, J.B., Kober, H., and Grummich, P. (1996). Sources of spontaneous slow waves associated with brain lesions, localized by using the MEG. Brain Topogr. 8, 215–221.
129. de Jongh, A., Baayen, J.C., De Munck, J.C., Heethaar, R.M., Vandertop, W.P., and Stam, C.J. (2003). The influence of brain tumor treatment on pathological delta activity in MEG. Neuroimage 20, 2291–2301.
130. Lewine, J.D., and Orrison, W.W., Jr. (1995). Spike and slow wave localization by magnetoencephalography. Neuroimaging Clin. N. Am. 5, 575–596.
131. Scheeringa, R., Petersson, K.M., Kleinschmidt, A., Jensen, O., and Bastiaansen, M.C. (2012). EEG alpha power modulation of fMRI resting-state connectivity. Brain Connect. 2, 254–264.
132. De Munck, J.C., Goncalves, S.I., Mammoliti, R., Heethaar, R.M., and Lopes da Silva, F.H. (2009). Interactions between different EEG frequency bands and their effect on alpha-fMRI correlations. Neuroimage 47, 69–76.
133. Hindriks, R., and van Putten, M.J. (2013). Thalamo-cortical mechanisms underlying changes in amplitude and frequency of human alpha oscillations. Neuroimage 70, 150–163.
134. Brookes, M.J., Hale, J.R., Zumer, J.M., Stevenson, C.M., Francis, S.T., Barnes, G.R., Owen, J.P., Morris, P.G., and Nagarajan, S.S. (2011). Measuring functional connectivity using MEG: methodology and comparison with fcMRI. Neuroimage 56, 1082–1104.
135. Brookes, M.J., Woolrich, M., Luckhoo, H., Price, D., Hale, J.R., Stephenson, M.C., Barnes, G.R., Smith, S.M., and Morris, P.G. (2011). Investigating the electrophysiological basis of resting state networks using magnetoencephalography. Proc. Natl. Acad. Sci. U.S.A. 108, 16,783–16,788.
136. Scholvinck, M.L., Leopold, D.A., Brookes, M.J., and Khader, P.H. (2013). The contribution of electrophysiology to functional connectivity mapping. Neuroimage 80, 297–306.
137. Scholvinck, M.L., Maier, A., Ye, F.Q., Duyn, J.H., and Leopold, D.A. (2010). Neural basis of global resting-state fMRI activity. Proc. Natl. Acad. Sci. U.S.A. 107, 10,238–10,243.
138. Shmuel, A., and Leopold, D.A. (2008). Neuronal correlates of spontaneous fluctuations in fMRI signals in monkey visual cortex:

Implications for functional connectivity at rest. Hum. Brain Mapp. 29, 751–761.
139. Nir, Y., Mukamel, R., Dinstein, I., Privman, E., Harel, M., Fisch, L., Gelbard-Sagiv, H., Kipervasser, S., Andelman, F., Neufeld, M.Y., Kramer, U., Arieli, A., Fried, I., and Malach, R. (2008). Interhemispheric correlations of slow spontaneous neuronal fluctuations revealed in human sensory cortex. Nat. Neurosci. 11, 1100–1108.
140. He, B.J., Snyder, A.Z., Zempel, J.M., Smyth, M.D., and Raichle, M.E. (2008). Electrophysiological correlates of the brain's intrinsic large-scale functional architecture. Proc. Natl. Acad. Sci. U.S.A. 105, 16,039–16,044.
141. Hyafil, A., Giraud, A.-L., Fontolan, L., and Gutkin, B. (2015). Neural cross-frequency coupling: connecting architectures, mechanisms, and functions. Trends Neurosci. 38, 725–740.
142. Lisman, J.E., and Jensen, O. (2013). The θ-γ neural code. Neuron 77, 1002–1016.
143. Knapp, C.H., and Carter, C.G. (1976). The generalized correlation method for estimation of time delay. IEEE Trans. Acoust. 21, 320–327.

Address correspondence to:
Ming-Xiong Huang, PhD
Radiology Imaging Laboratory
University of California at San Diego
3510 Dunhill Street
San Diego, CA 92121

E-mail: mxhuang@ucsd.edu